

WaterFEL: PROJECT UPDATE ON THE NEW CANADIAN INFRARED FREE ELECTRON LASER FACILITY

M. Boland^{1*}, N. Ayala², H. Bluem³, B. Bromberger², M. Ditty⁴,
K. Dunkel², S. Gottschalk⁵, S. Hopkins⁴, C. Ieritano⁴,
J. Rathke⁶, W. Schöllkopf⁷, X. Stragier⁸, A. Todd⁹, A. van Vliet¹⁰, L. Young⁴

¹University of Saskatchewan, Saskatoon, Canada

²RI Research Instruments GmbH, Germany

³Private Consultant, ⁴University of Waterloo, Waterloo, Canada

⁵STI Magnetics, ⁶JW Rathke Engineering Services

⁷Fritz Haber Institute of the Max Planck Society, Germany

⁸Canadian Light Source, Canada, ⁹AMMTodd Consulting

¹⁰Radboud University Nijmegen, Nijmegen, The Netherlands

Abstract

The WaterFEL is a national Infrared Free Electron Laser (IR FEL) facility that is funded and currently under development. Ground breaking for the new building that will house the facility has taken place at the University of Waterloo, Ontario, Canada. A design based on a similar facility at the Fritz Haber Institute in Berlin is being adapted for the WaterFEL accelerator and beamlines. The IR FEL machine will consist of an electron linac with energy up to 50 MeV and two undulators to create light for two beamlines, one in mid IR and one in far IR. The major components are currently being procured and should be completed by 2027. This is a brief report on the project and some of the design parameters.

BACKGROUND

The Canadian scientific community has a strong expertise in IR science and a long history of using international FELs to do their research. This community has driven the motivation for Canada to build its own national IR FEL facility with a big push culminating in a whitepaper that formed the basis of grant application [1]. The purpose of the lab is to expand the excellent science knowledge that has come from accelerator based national facilities in Canada and compliment the existing facilities with new capabilities. The WaterFEL project [2] has now been funded and is currently in the process of constructing the building that will house the facility and busy constructing and procuring the hardware for the machine. The facility is being constructed in the innovation precinct of the University of Waterloo in the province of Ontario and an architectural rendering of the building is shown in Fig. 1. A preliminary design of the machine is shown in Fig. 2.

The goal of the facility is to be a national science user facility open to merit based proposals for beamtime. IR light in spectral range from 3 to 175 μm (3333 to 57 cm^{-1} wavenumbers) with up to 20 Hz repetition frequency of a 3–18 μs macropulses that contain a 1 GHz pulse train of 1 to

5 ps long bunches will be delivered to several experimental end stations. The design of the facility is based mainly on similar ones in Germany at FHI — which has just achieved two colour operation [3] — and The Netherland at FELIX, which has been in operation since the 1990s [4].

CONTEXT

Canada has a history of accelerator based science facilities [5], including the TRIUMF heavy ion nuclear facility and the CLS synchrotron radiation facility. While CLS does have an IR beamline [6], this provides a less intense and longer timescale beam that is complimentary to the WaterFEL design.

Future applications at WaterFEL include vibrational spectroscopy for the identification and characterization of molec-



Figure 1: WaterFEL building architectural render.

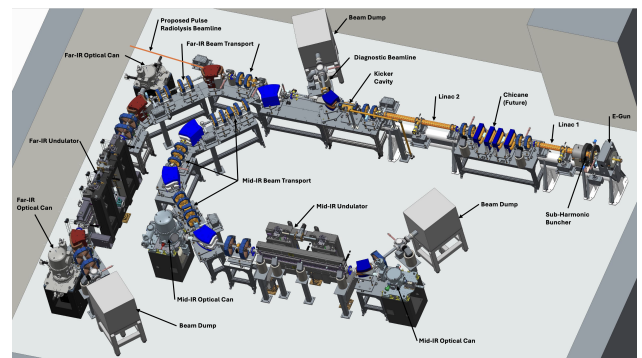


Figure 2: WaterFEL machine CAD render.

* email: mark.boland@usask.ca

ular fingerprints, enabling sensitive detection of disease biomarkers and emerging environmental contaminants, as well as Infrared and THz imaging of biological tissues and quantum materials with chemical and spatial specificity. These experiments will provide insight into low-energy excitations, collective modes and transport phenomena. There will be an advanced electron diffraction end-station to enable structural characterization of condensed matter systems, inorganic clusters and isolated gas-phase molecules including complex biomolecules such as proteins—revealing transient and equilibrium structural detail. When coupled with the FEL, these end-stations can be used for time-resolved pump–probe experiments, allowing direct observation of ultrafast molecular and material dynamics, including energy transfer, conformational change, phase transitions and non-equilibrium processes. Integration with cryogenic spectrometers further permits the study of molecular structure, weak intermolecular interactions and reaction precursors under ultracold conditions with exceptional spectral resolution.

The WaterFEL facility will fill a gap in the Canadian scientific infrastructure landscape and compliment other facilities in operation and under construction in Canada. The funding for the facility was provided in part by the CFI and the grant also included support for a project to create THz radiation at TRIUMF using a branch line of their 30 MeV SRF electron linac [7]. Some of the Canadian collaborators and other IR FEL facilities in operation are listed below.

Canadian Collaboration

On the machine side, there is an active group of researchers at TRIUMF and CLS who are supporting the design and simulations of the accelerator systems. This includes work on both the WaterFEL facility and the TRIUMF THz branch line at ARIEL, which also plans to develop a user facility. On the beamline side, there is an active group of researchers at Canadian universities who are providing the motivation for science capability and supporting the project. These Canadian facilities will enable better access to research infrastructure and provide more opportunities to train young scientists in the use of accelerator based light sources and in accelerator physics and engineering.

Other Facilities

The WaterFEL facility will join a global community of IR FEL facilities that are in operation, a selected list of those that are well known is shown in Table 1. Most of the facilities are in Europe and Japan, so WaterFEL will fill a gap in the capacity of IR sources in the Americas.

DESIGN

Accelerator Layout

The basic layout of the accelerator systems are shown in Fig. 3. A 90 keV dispenser cathode thermionic gun, with a grid modulated at 1 GHz is put through a series of solenoids, in between which is a 1 GHz bunching cavity. The bunched beam is injected into two 2.998 GHz standing wave

linacs with a final maximum energy of the electron beam of 50 MeV. A space is left between the two linacs for the possible installation of a magnetic chicane in the future, which will enable the control of the longitudinal bunch length at the undulators using longitudinal compression.

Accelerator Parameters

A list of accelerator parameters and performance goals of WaterFEL are shown in Table 2. A pulser on the electron gun HV deck will enable micropulse operation from 55 MHz to the nominal 1 GHz electron bunch repetition rate.

Undulator Parameters

The undulators are designed to produce a spectrum of 3–175 μm . The peak field (K_{rms}) for the 40 mm period Mid-IR undulator will be 0.614 T ($K_{\text{rms}} = 1.62$) at a gap of 16.5 mm. The Far-IR undulator with a period of 68 mm will have a peak field (K_{rms}) of 0.496 T ($K_{\text{rms}} = 2.23$) at a gap of 32 mm. The radiation resistant, wedged pole hybrid design by STI Magnetics will be built and measured onsite at the University of Waterloo in a magnet mapping lab that is presently under construction. A list of nominal beamline parameters are listed in Table 3.

Optical Transport Systems

The optical cavities of each FEL are both 5.4 m long, to ensure correlation between both for two-color experiments, with up to 36 electron bunches circulating in the cavity at one time — 36 for 1 GHz single FEL and 2 for 55.5 MHz operation. One optical chamber houses a reflecting mirror whose axial length can be finely adjusted to control the cavity detuning while the other contains 4 interchangeable mirrors with different diameter small outcoupling holes followed by Brewster angle diamond outcoupling windows. Two optical transport ISO-K 100 pipes carry the FEL radiation from the bunker to an optical diagnostic room next to the control room on the ground floor where the power and spectra of the radiation is analyzed. Two output optical transport trunk lines then carry and distribute the radiation to experiments in the proximate experimental Ballroom Laboratory.

ACCELERATOR SIMULATIONS

End-to-End Accelerator Simulation

The accelerator was simulated from the cathode to the end of linac 2 in order to demonstrate the transmission, energy, energy spread and beam envelope. The code TStep [20] was used to track particles from the cathode surface that were first modulated by a 1 GHz RF signal on the grid. This simulated the initial bunching of the beam, before it was focused by the gun solenoid. A 1 GHz Sub-Harmonic Buncher cavity was then used to compress the bunch longitudinally, before being focused transversely using four more solenoids. Figure 4 shows the new design for the gun that was used in the end-to-end simulations.

The solenoids were adjusted in position and current strength to create a near parallel beam at the entrance to

Table 1: Selected list of IR FEL facilities worldwide. See Ref. [8] for a more exhaustive list of FELs of all energies.

Facility	C'try	Status	Wavelength (μm)	Wavenumber (cm^{-1})
CLIO (Université Paris-Saclay) [9]	FR	User facility	5 – 150	67 – 2000
FELIX (Radboud University) [10]	NL	User facility	3 – 250	40 – 3333
Fritz Haber Institute IR-FEL [11]	DE	Operational	3 – 160	63 – 3333
FELBE (HZDR, Dresden-Rossendorf) [12]	DE	User facility	4 – 250	40 – 2500
FELI (FEL Research Institute, Osaka) [13]	JP	Operational	5 – 300	33 – 2000
ISIR FEL (Osaka University) [14]	JP	Operational	5 – 20	500 – 2000
KU-FEL (Kyoto University) [15]	JP	Operational	5 – 20	500 – 2000
IR-FEL at RRCAT [16]	IN	Operational	12.5 – 50	200 – 800
Chiang Mai University IR-FEL [17]	TH	Operational	3 – 10	1000 – 3333
TARLA IR-FEL at TAC [18]	TR	Early operation	3 – 30	333 – 3333
WaterFEL (University of Waterloo)	CA	Under construction	3 – 175 (design)	57 – 3333
PolFEL (Świerk) [19]	PL	Under construction	60 – 600	17 – 167

WaterFEL Accelerator Layout

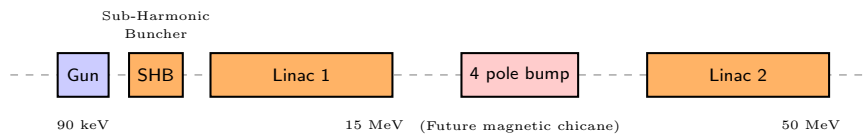


Figure 3: Layout diagram of the accelerator systems for WaterFEL.

Table 2: Parameter Table for the Electron Accelerator

Parameter	Value
Electron Energy	15–50 MeV
Electron Source Energy	90 keV
Bunch charge	220 pC
Bunch length	1 to 5 ps
Macropulse length	3–18 μs
Bunch frequency	1 GHz, 55.5 and 111 MHz
Macropulse frequency	1–20 Hz
Linac frequency	2.998 GHz

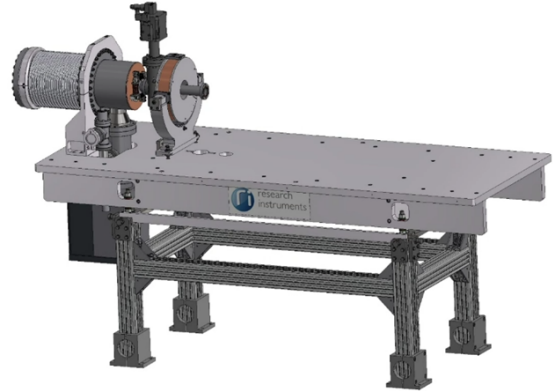


Figure 4: New design for the electron gun, to replace the FHI system shown in Fig. 2.

Table 3: Parameter Table for the Mid-IR and Far-IR Undulators

Parameter	Mid-IR	Far-IR
Type	Wedged Pole	Planar hybrid
Material (NdFeB)	Vacodym 890TP	983DTP
Period	40 mm	68 mm
Length	2.026 m	2.219 m
# Periods (useful)	51 (49)	33 (30)
K_{RMS}	0.3–1.62	0.3–2.23
Wavelength range	3–60 μm	5–175 μm
Wavenumber range	167–3333 cm^{-1}	57–2000 cm^{-1}
Frequency range	5–100 THz	1.7–60 THz
Cavity Length	5.4 m	5.4 m
Bandwidth	0.45% $\Delta\lambda/\lambda$	0.45% $\Delta\lambda/\lambda$

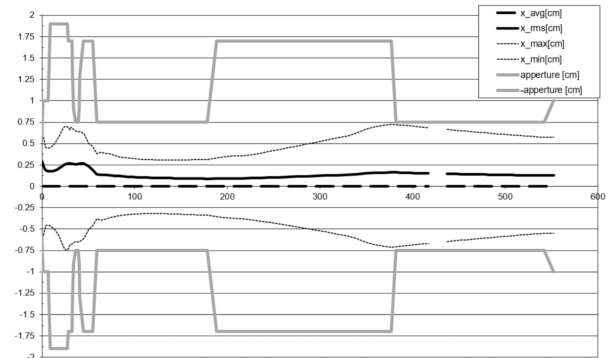


Figure 5: Beam envelope from TStep simulations.

linac 1. The simulation results achieve a beam energy of 50.1 MeV with an energy spread of $\Delta E = 0.1\%$ after applying a filter which results in a transmission efficiency of

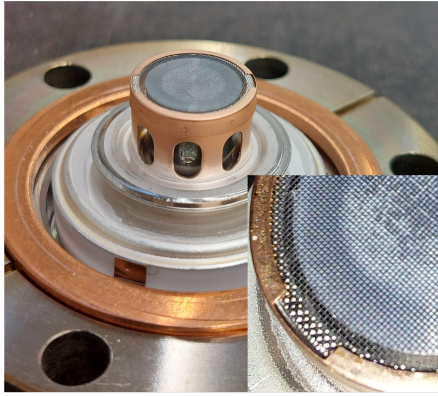


Figure 6: Photo of a used and decommissioned cathode from FELIX.

97.8%, with 224 pC charge in the bunch and a length of 2.1 ps. The end-to-end beam profile is shown in Fig. 5 to be within the physical aperture for the maximum amplitude particles. The simulated emittance was $13 \text{ mm} \cdot \text{mrad}$. Work is ongoing for the final design of the accelerator before manufacturing will begin.

Detailed Gun Simulation

To simulate the gun, a model was developed to first calculate the fields using a detailed geometry of the cathode. A used and decommissioned cathode was used as the basis for the model and Fig. 6 shows the assembly in the flange and an inset showing the detail of the grid in front of the cathode. The grid and cathode were also examined under a scanning electron microscope (SEM) and the composite image is shown in Fig. 7. There are signs of the formation of a distinct inner circular region which is shown in SEM spectral analysis to contain barium (Ba), known for its low work function and as a good electron emitter, as well as tungsten (W) which is a common substrate for constructing cathodes. It is assumed that the reduction of the perveance, commonly observed over the lifetime of a cathode, is related to the formation of this smaller radius inner circle which was the dominant emission surface before the cathode was replaced.

The basic circuit diagram of the gun is shown in Fig. 8. Initially, the bias voltage was set to $V = -9 \text{ V}$ relative to the cathode, so the electrons that are ionised due to the temperature experience a negative potential gradient and are forced back towards the cathode. Figure 9 shows the E-field at the cathode reverses direction at the cathode surface with a bias voltage of -9 V compared to when there is zero bias voltage. Note also the distortion of the fields around the circular cross section of the wires from the grid shown pointing out of the page. In this model, the perpendicular wires shown here in the vertical direction are in the same plane as those coming out of the page, whereas in the physical device they are interwoven — a detail not deemed critical to include for this iteration of the simulation.

The beam can be switched on by applying a negative bias voltage pulse to the cathode, typically for a time $\Delta t \approx$

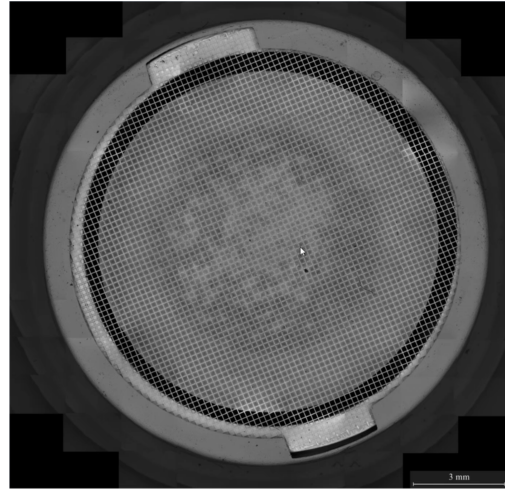


Figure 7: SEM image of the grid in front of the thermionic dispenser cathode. Credits: Cathode from FELIX, SEM image from CLS (Image: Burke Barlow).

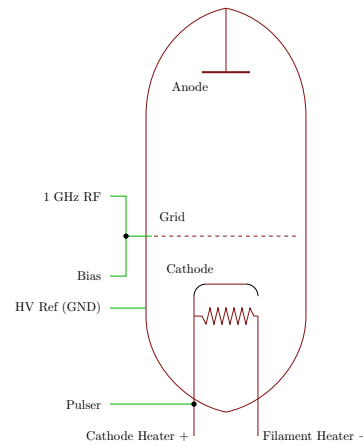


Figure 8: Basic circuit diagram of the gun showing the anode and cathode with the grid and the bias, pulser and RF voltage connections.

$3\text{--}18 \mu\text{s}$, which is in turn modulated by the 1 GHz RF voltage. The pulse voltage is adjusted so that by itself will not cause emission, except at a small phase range at the peaks of the sinusoidal RF wave.

The initial end-to-end simulations took into account the RF modulation of the gun grid, however only the fields were applied as if it were a flat transparent plate and not the details of the grid wires. A separate simulation was performed that took into account both the distortions of the RF fields due to the wire structure and the loss of particles that were emitted from the cathode but then absorbed when hitting the grid wires. The distortion of the fields due to the wires resulted in an increase in the beam emittance of a factor of 3. In addition, both Child's Law [21] and Richardson's Law [22] were taken into account for the simulations, to get a feel for what realistic bunch charge can be achieved.

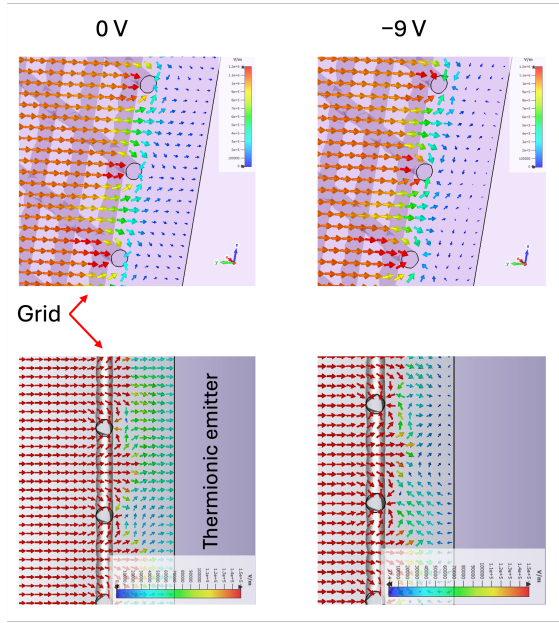


Figure 9: CST simulation of the E-fields between the grid and the cathode with and without the bias voltage used to suppress emission.

Child's Law relates the maximum current in A from a cathode to the applied voltage as:

$$I = PV^{3/2}, \quad (1)$$

where P is the perveance of the gun which depends of the geometry, given by

$$P = \frac{4}{9} \epsilon_0 A \sqrt{\frac{2e}{m_e}} \frac{1}{d^2}, \quad (2)$$

where d is the cathode-anode spacing and A the cathode emitting area.

Richardson's Law related the temperature T , the electric field gradient E and the cathode material work function $\Delta\phi$ to the current density as

$$J(T, E, \Delta\phi) = A_R T^2 \exp\left(-\frac{(\phi - \Delta\phi)}{k_B T}\right), \quad (3)$$

where $\Delta\phi$ and A_R are

$$\Delta\phi = \sqrt{\frac{e^3 E}{4\pi\epsilon_0}} \text{ and } A_R = \frac{4\pi m e k_B^2}{h^3}, \quad (4)$$

and for area of emission A

$$I_{\text{emitted}} = A A_R T^2 \exp\left(-\frac{(\phi - \Delta\phi)}{k_B T}\right). \quad (5)$$

The exact temperature is not known for this particular setup, however from the literature a typical temperature is around 1000°C [23, p. 543]. These equations were used to correctly modify the maximum current that can be extracted with the -90 kV high voltage from the gun design. The

currents were converted into the corresponding charges used in the macro particles that were tracked through the fields in the gun. The GPT code [24] was used for particle tracking simulations and in addition to importing the fields calculated in CST, the wire mesh was stipulated as a region in which to discontinue tracking, when electrons impinged on these regions. This way it was possible to get both an estimate of the emittance growth due to the non-parallel fields resulting from the grid, as well as the screening effect and hence the efficiency of transmission of beam from the cathode to the other side of the grid.

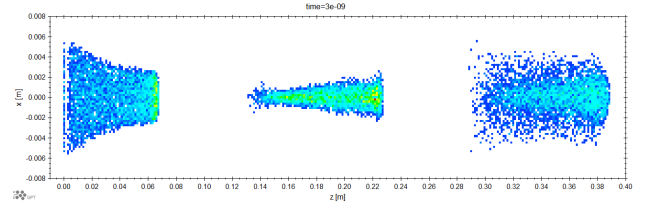


Figure 10: Simulation of detailed gun model with particle tracking in GPT.

The simulation results show in Fig. 10 show the clear formation of the bunch structure from the cathode due to the RF applied between the grid and the emitter. At $z = 0.00\text{ m}$ a thin vertical line shows the gap created at the end of one bunch, where the line or particles to the left is sent back towards the emitter surface as the RF phase changes and the field reverses direction. The effect of the solenoid focusing starting at $z = 0.234\text{ m}$ can also be seen by the change in transverse size from one bunch to the next. Once this model has been fully implemented with the final design, it will be used to try to optimise the system for various operational modes using a multi-objective genetic algorithm.

CONCLUSION

The WaterFEL project is funded and well underway to building a new national scientific user facility for Infrared experiments. The design is currently being finalised and the new building has started construction on the campus of the University of Waterloo.

Simulations have been performed to verify the initial design of the accelerator. Undulator designs have been completed and a magnetics lab is being installed to complete the build and measurements these devices.

Installation of the equipment is planned for early 2027, with first light in mid-2027 and first expert users experiments in early 2028.

ACKNOWLEDGEMENTS

The authors would like to thank the funders CFI, University of Waterloo, BC Knowledge Development Fund (BCKDF), Ontario Research Fund (ORF) and Natural Sciences and Engineering Research Council of Canada (NSERC) and our collaborators at FHI, FELIX, TRIUMF, CLS (Bourke Burlow, SEM images).

REFERENCES

- [1] W. S. Hopkins, V. Verzilov, G. Sciaini, I. Burgess, and M. Boland, “Establishing a canadian free-electron laser research program”, *Can. J. Phys.*, vol. 97, no. 12, pp. vii–x, Dec. 2019. doi:10.1139/cjp-2019-0238
- [2] University of Waterloo, WaterFEL – waterloo free electron laser facility, <https://uwaterloo.ca/waterloo-free-electron-laser-facility/>
- [3] W. Schöllkopf *et al.*, “A two-color dual-oscillator infrared free-electron laser”, *arXiv*, 2026. doi:10.48550/arXiv.2604.16189
- [4] D. Oepts, A. FG. van der Meer, and P. W. van Amersfoort, “The Free-Electron-Laser user facility FELIX”, *Infrared Phys. Technol.*, vol. 36, no. 1, pp. 297–308, 1995. doi:10.1016/1350-4495(94)00074-U
- [5] M. K. Craddock and R. E. Laxdal, “Accelerator science and technology in Canada — From the Microtron to TRIUMF, superconducting cyclotrons and the Canadian Light Source”, *Rev. Accel. Sci. Technol.*, vol. 08, pp. 225–267, 2015. doi:10.1142/S1793626815300121
- [6] T. May, T. Ellis, and R. Reininger, “Mid-infrared spectro-microscopy beamline at the canadian light source”, *Nucl. Instrum. Methods Phys. Res. A*, vol. 582, no. 1, pp. 111–113, 2007. doi:10.1016/j.nima.2007.08.074
- [7] S. R. Koscielniak *et al.*, “TRIUMF ARIEL e-Linac ready for 30 MeV”, in *Proc. IPAC'17*, Copenhagen, Denmark, May 2017, pp. 1361–1364. doi:10.18429/JACoW-IPAC2017-TUPAB022
- [8] P. J. Neyman, J. Blau, K. R. W. B. Colson, S. C. Gottschalk, and A. M. M. Todd, “Free electron lasers in 2017”, in *Proc. FEL'17*, Santa Fe, NM, USA, Aug. 2017, pp. 204–209. doi:10.18429/JACoW-FEL2017-MOP066
- [9] F. Glotin *et al.*, “First lasing of the CLIO FEL”, in *Proc. EPAC'92*, Berlin, Germany, Mar. 1992, pp. 620–623. https://proceedings.jacow.org/e92/PDF/EPAC1992_0620.PDF
- [10] P. W. van Amersfoort, R. J. Bakker, C. A. J. V. der Geer, and A. F. G. V. der Meer, “Commissioning the electron accelerator for FELIX”, in *Proc. EPAC'90*, Nice, France, Jun. 1990, pp. 547–550. https://proceedings.jacow.org/e90/PDF/EPAC1990_0547.PDF
- [11] A. M. M. Todd *et al.*, “The FHI FEL upgrade design”, in *Proc. IPAC'19*, Melbourne, Australia, May 2019, pp. 1903–1905. doi:10.18429/JACoW-IPAC2019-TUPRB103
- [12] P. Michel *et al.*, “The Rossendorf IR-FEL ELBE”, in *Proc. FEL'06*, Berlin, Germany, Aug.-Sep. 2006, paper TUCAU02, pp. 488–491, 2006. <https://jacow.org/f06/papers/TUCAU02.pdf>
- [13] T. Tomimasu *et al.*, “Operation of FIR- and UV-FEL facilities and FEL beam sharing to user’s rooms at the FELI”, in *Proc. PAC'97*, Vancouver, Canada, May 1997, pp. 730–732. <https://ieeexplore.ieee.org/stamp/stamp.jsp?arnumber=749818>
- [14] K. Kawase *et al.*, “High power operation of the THz FEL at ISIR, Osaka University”, in *Proc. FEL'14*, Basel, Switzerland, Aug. 2014, pp. 528–531. <https://jacow.org/FEL2014/papers/TUP073.pdf>
- [15] T. K. H. Zen and H. Ohgaki, “Present status of Kyoto University Free-Electron Laser facility, KU-FEL”, in *Proc. IPAC'23*, Venice, Italy, May 2023, pp. 1866–1869. doi:10.18429/JACoW-IPAC2023-TUPL050
- [16] S. Chandran *et al.*, “The IR-FEL facility at RRCAT: Commissioning experiments and first saturation of lasing at 28 μm wavelength”, *Nucl. Instrum. Methods Phys. Res. A*, vol. 1003, p. 165321, 2021. doi:10.1016/j.nima.2021.165321
- [17] S. Rimjaem *et al.*, “Infrared free-electron laser project in Thailand”, in *Proc. IPAC'22*, Bangkok, Thailand, Jun. 2022, pp. 1070–1073. doi:10.18429/JACoW-IPAC2022-TUPOPT029
- [18] A. Aksoy, Ö. K. Ç. Kaya, İ. B. Koç, and Ö. F. Elçim, “Current status of free electron laser @ TARLA”, in *Proc. FEL'19*, Hamburg, Germany, Aug. 2019, pp. 102–105. doi:10.18429/JACoW-FEL2019-TUP025
- [19] W. Grabowski, “PoLFEL – Polish free electron laser under construction”, presented at IPAC'24, Nashville, TN, USA, May 2024, paper MOPG35, unpublished.
- [20] L. M. Young and J. Billen, “The particle tracking code PARMELA”, in *Proc. PAC'03*, Portland, OR, USA, May 2003, pp. 3521–3523. doi:10.1109/pac.2003.1289968
- [21] C. D. Child, “Discharge from hot CaO”, *Phys. Rev. (Series I)*, vol. 32, no. 5, pp. 492–511, May 1911. doi:10.1103/PhysRevSeriesI.32.492
- [22] O. W. Richardson, *The Emission of Electricity from Hot Bodies*. London, UK: Longmans, Green and Co., 1921.
- [23] A. W. Chao, K. H. Mess, M. Tigner, and F. Zimmermann, *Handbook of Accelerator Physics and Engineering*. Singapore, World Scientific, 2013. doi:10.1142/8543
- [24] Pulsar Physics, General particle tracer (GPT), <https://www.pulsar.nl/gpt>